

Available online at www.sciencedirect.com
SciVerse ScienceDirect
www.elsevier.com/locate/jmbbm

Puncture resistance of the scaled skin from striped bass: Collective mechanisms and inspiration for new flexible armor designs

 Deju Zhu^a, Lawrence Szewciw^a, Franck Vernerey^b, Francois Barthelat^{a,*}
^aDepartment of Mechanical Engineering, McGill University, Montreal, QC, Canada

^bDepartment of Civil, Environmental and Architectural Engineering, University of Colorado, Boulder, CO, USA

ARTICLE INFO

Article history:

Received 1 March 2013

Accepted 13 April 2013

Available online 22 April 2013

Keywords:

Striped bass (*Morone saxatilis*)

Teleost

Fish skin

Fish scale

Scalation pattern

Puncture resistance

Biomimetics

Body armor

ABSTRACT

The structure and mechanics of fish scales display unusual and attractive features which could inspire new protective materials and systems. This natural material is therefore attracting attention over the past few years, and recent work demonstrated the remarkable performance of individual fish scales. A puncture event as would occur from a predator's attack however involves more than one scale, and in this article we therefore investigate collective mechanisms occurring within the scaled skin of a fish in the event of a predator's attack. We first demonstrate that in striped bass (*Morone saxatilis*), the scales increase by four to five times the force required to puncture the skin. We show that individual scales from striped bass provide a remarkable barrier against sharp puncture, regardless of the stiffness of the substrate. The scalation pattern in striped bass is such that three scales overlap at any point on the surface of the fish, which we show effectively multiplies the puncture force by three. We determined that the friction between scales is negligible and therefore it does not contribute to increasing puncture force. Likewise, we found that the local arrangement of the scales had little effect on the puncture performance. Interestingly, because the scales are several orders of magnitude stiffer than the substrate, indenting a few isolated scales results in "sinking" of the scales into the substrate. The high local deflections and strain within the soft tissue may then result in blunt injury before the sharp indenter penetrates the scales. Stereo-imaging and image correlation performed around a puncture site in fish reveal that the surrounding scales collectively contribute to redistributing the puncture force over large volume, limiting local deflections and strains in the soft tissues. The structure and mechanisms of natural fish scales therefore offer an effective protection against several types of threat, and may inspire novel versatile protective systems with attractive flexural properties.

© 2013 Elsevier Ltd. All rights reserved.

1. Introduction

Natural materials and organisms are increasingly serving as inspiration for novel solutions to engineering problems.

In particular, there is a growing interest in examining how animals evolve protective systems against predators or other mechanical threats (Meyers et al., 2012; Yang et al., 2013). The scaled skin of fish is a 500 million-year-old protective system,

*Corresponding author. Tel.: +1 514 398 6318; fax: +1 514 398 7365.

E-mail addresses: deju.zhu@mail.mcgill.ca (D. Zhu), lawrence.szewciw@mail.mcgill.ca (L. Szewciw), franck.vernerey@colorado.edu (F. Vernerey), francois.barthelat@mcgill.ca (F. Barthelat).

with many attributes which would be desirable in personal protective systems: it is ultrathin, flexible, light weight, transparent, breathable, and can resist puncture from collision with obstacles or other fish, or from attacks by predators (Elliott, 2000). In an effort to better understand this natural system, a number of recent articles have focused on the structure and mechanics of individual fish scales. Tensile tests have revealed the scale's capability to absorb large deformation and energy, associated with progressive failure mechanisms (Ikoma et al., 2003; Torres et al., 2008; Zhu et al., 2012; Garrano et al., 2012). Energy dissipative mechanisms were also studied in detail for ganoid scales from the "pre-historic" fish *Polypterus senegalus*, using nanoindentation techniques (Bruet et al., 2008). More recently, sharp puncture tests were used in order to measure the force required to completely defeat the scale, using a sharp needle (Zhu et al., 2012) or even actual teeth of predators (Meyers et al., 2012). The high puncture resistance of teleost fish scales was demonstrated by Zhu et al. (Zhu et al., 2012), and explained by a two-step failure associated with the bony and collagen layers of the scale. We now have a good understanding of the structure and mechanisms associated with the deformation, fracture and puncture of the three major fish scale types (teleost, cosmoid and ganoid) as individual components. The protective layer provided by natural fish skin consists of many scales, and while the structure and scalation or squamation patterns of various fish scales is now well documented (Elliott, 2000; Meunier and Castanet, 1982; Burdak, 1979), little is known on how scales interact to generate high resistance to puncture. The mechanical interaction between teleost scales upon puncture or bending of

the fish was modeled by Vernerey and Barthelat (Vernerey and Barthelat, 2010) and suggests that interaction between the scales can enhance both penetration resistance and locomotion by increasing flexural stiffness, providing an exotendon effect during swimming as well as dispersing puncture force and preventing unstable localized deformation during puncture. More recently, Browning et al. (Browning et al., in press) studied scale-scale interactions during puncture using a two-dimensional polymer model of elasmoid scales, revealing useful mechanisms and properties associated with the scalation pattern. In this work, we report, for the first time, insights into collaborative mechanisms between scales during a puncture event on natural fish skin. The main goal of this work was to identify key mechanisms and parameters controlling the puncture resistance of fish skin, in order to ensure an efficient biomimetic "transfer of technology" to synthetic flexible protective systems.

2. The structure of fish skin

The structure of individual scales and their arrangement (scalation pattern) were characterized for striped bass (*M. saxatilis*), a common teleost fish originating from the northern Atlantic Ocean. The specimens we used for this work originated from the fish supplier, Nature's Catch Inc., Clarksdale, MS, USA. The majority of the body of the fish is covered by scales (Fig. 1a). A detailed analysis of the scalation pattern revealed that in striped bass the scales are arranged in rows along the length of the fish. Each scale overlaps with six other neighboring scales: three scales on the anterior side, and

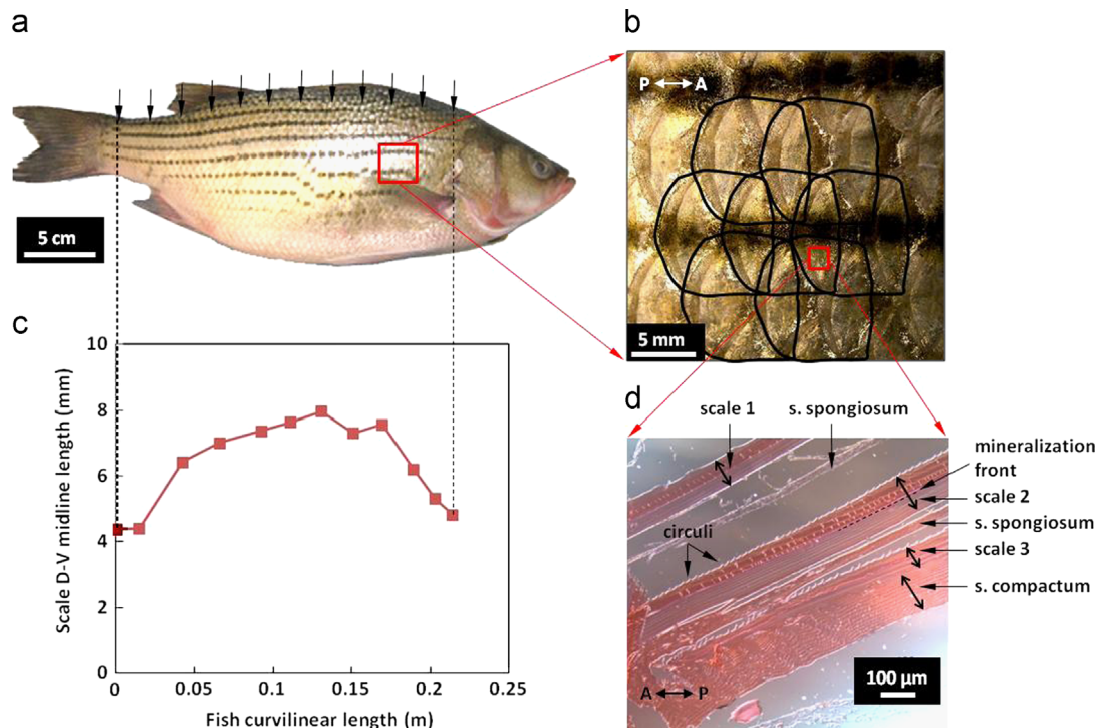


Fig. 1 – (a) Whole striped bass; (b) detail of the scalation pattern: the central scale covers three posterior (P) scales and is covered by three anterior (A) scales, resulting in three scale overlap at any location on the skin; (c) dimensions of individual scales along the length of the fish; (d) histological cross section showing three scale overlap (H&E stain).

three scales on the posterior side (Fig. 1b). Interestingly, the arrangement of the scales is such that any point on the surface of the fish is covered by three overlapping scales. The scales are however not uniform in size over the entire fish. For example, Fig. 1c shows the variation of scale diameter along the dorsal line of the fish. The scales are the smallest near the tail and near the head, and that they can be up to twice as large at a distance of about 1/3 of the fish length from the head. The absolute size of individual scales varies in dimensions with the age of the fish (fishes keep growing indefinitely so that there is no “adult size”) (Elliott, 2000). Fig. 1d shows a histological section of the skin of striped bass, prepared with H&E staining. The section shows three overlapping dermal scales with a softer, gel-like connective tissue (called stratum (s.) spongiosum, (Elliott, 2000)) between the scales. The underlying dermal tissue, called s. compactum (Elliott, 2000), is a 100–200 μm thick dense layer of collagen fibrils in which the scales are anchored (Fig. 1d). The s. compactum, which exhibits a cross-helical arrangement of collagen fibers, has typically been proposed to function in stretch resistance and in locomotion via an exotendon effect (Elliott, 2000; Motta, 1977; Wainwright et al., 1978; Hebrank and Hebrank, 1986; Whitear, 1986; Naresh et al., 1997), but has also been implicated in improving penetration resistance, at least in sharks (Motta, 1977). Each individual scale is 200–400 μm thick, and composed of collagen type I fibrils (Zhu et al., 2012). The outer “bony” (calcified) layer represents about one half of the thickness and is mineralized with hydroxyapatite (HAp) (Elliott, 2000; Zhu et al., 2012; Whitear, 1986; Schonborner et al., 1979), as revealed here with the selective H&E and von Kossa staining (Fig. 1d). The collagen fibrils of the inner “collagen” layer are arranged in a plywood pattern with the lamellae consisting of parallel fibrils that rotate across lamellae by angles that vary between species (Zhu et al., 2012; Meunier and Castanet, 1982), the plywood pattern increasing strength in multiple directions (Ikoma et al., 2003; Torres et al., 2008; Zhu et al., 2012). Fig. 1d also shows cross sections of the intricate roughness patterns

(called circuli with denticles) covering the outer surface of the scales, which may provide mechanical anchoring of the scale (Elliott, 2000; Zhu et al., 2012; Lanzing and Higginbotham, 1974; Sire, 1986).

We also characterized the three-dimensional morphology of individual scales using micro-computed tomography (micro-CT). Fig. 2a shows the surface of the scale and clearly reveals surface features such as posterior ctenii (stiff projections with hydrodynamic functions) and anterior radii (radial grooves that may increase scale flexibility) (Elliott, 2000; Zhu et al., 2012; Sire, 1986). Fig. 2b shows a map of the scale thickness computed from the micro-CT scans. These data reveal that individual scales are thickest at the focal point on the scale (the “focus”), and that the thickness progressively decreases towards the edges of the scale. The pattern of thickness distribution conforms to the traditional sectors of the scale based on surface roughness (focus, lateral, anterior and posterior regions). When scales are superimposed the “effective” thickness of protective material is increased. Interestingly, examination of the scalation pattern (Fig. 1b) and the thickness distribution of individual scales (Fig. 2b) suggests that this “effective thickness” generated by superposing three scales, is uniform over the surface of the fish.

3. The puncture performance of fish skin

Although it is believed that the scaled skin of fish has multiple functions (Elliott, 2000), its primary role is probably protection against predators (Meyers et al., 2012; Yang et al., 2013; Elliott, 2000; Zhu et al., 2012; Bruet et al., 2008). To assess the effectiveness of scales, we therefore performed puncture experiments on whole fish skin to duplicate a predator's attack. A half-striped bass was placed in immersed condition and a sharp needle (tip radius = 35 μm) mounted on a universal testing machine was driven through the skin (Fig. 3a). Tests were performed on fully scaled fish as well as on entirely descaled fish for comparison. The results demonstrate that the scales provide a highly efficient

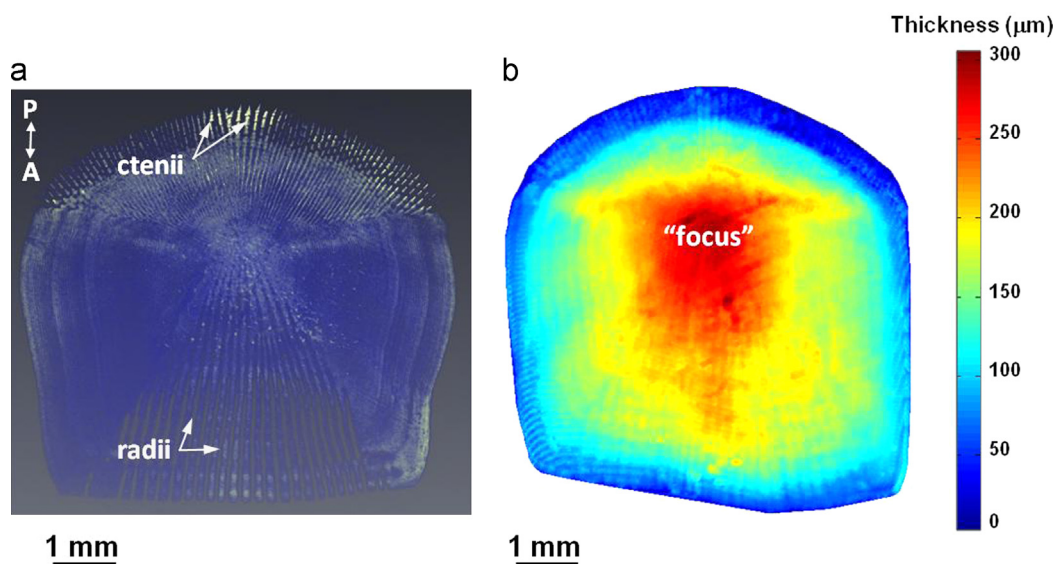


Fig. 2 – (a) Micro-CT image of an individual scale showing ctenii and radii (A-P=anteroposterior); (b) map of scale thickness obtained from micro-CT.

barrier against predators, increasing the puncture resistance of the skin by four to five times (Fig. 3b). The scales also stiffen the skin, with the effect of decreasing the amount of deflection upon puncture. In terms of biomimetics, it is critical to examine and identify the structure and mechanisms behind this performance. In a previous work we demonstrated that individual scales displayed a remarkably high resistance to sharp puncture, and we identified the structures and mechanisms associated with this performance (Zhu et al., 2012). The outer “bony” layer and inner “collagen” layer operate in synergy to trigger specific failure mechanisms which dissipate energy and increase the force required to completely puncture the scale (Zhu et al., 2012). Other potential effects influencing the puncture mechanics and performance of fish skin include substrate stiffness (dermis and flesh), puncture site, number of overlapping scales, friction between scales, scale arrangement, and long distance collaborative mechanisms between scales and force dispersal. These various aspects are systematically explored in the following sections.

4. Effect of substrate stiffness

The deflection and deformation of the scales is largely controlled by the stiffness of the underlying substrate, but it is not clear whether the substrate affects their puncture resistance.

More generally, the question of whether the structure and mechanics of fish scales have evolved in relation to the properties of the underlying tissue must be assessed for a proper biomimetic transfer to synthetic systems. In this section, we have investigated this question for natural fish, using puncture tests on individual fish scales resting on elastomeric substrates with different stiffnesses. Three substrates covering a wide range of stiffness were considered: a soft silicone rubber, a hard silicone rubber, and natural fish substrate dissected from striped bass consisting of the dermis (specifically descaled skin) and underlying muscle. These materials were cut into $2.5 \times 2 \times 1.5 \text{ cm}^3$ blocks which served as substrate for puncture tests on the individual fish scales. The elastic properties of each of these substrates were measured by spherical indentation, using a 3.16 mm steel probe. An inverse method was used to recover the elastic parameters of the substrates from the experiments: the indenter and substrate were modeled with finite elements (ANSYS Inc., Houston, Pennsylvania, USA) (Fig. 4a). Axisymmetric elements were used. The spherical indenter was assumed to be perfectly rigid, and frictionless contact elements were inserted between the indenter and the upper surface of the substrate. The substrate was modeled as a Neo-Hookean incompressible material because of its elastomeric nature. The finite element mesh was progressively refined until convergence of the force–displacement curves.

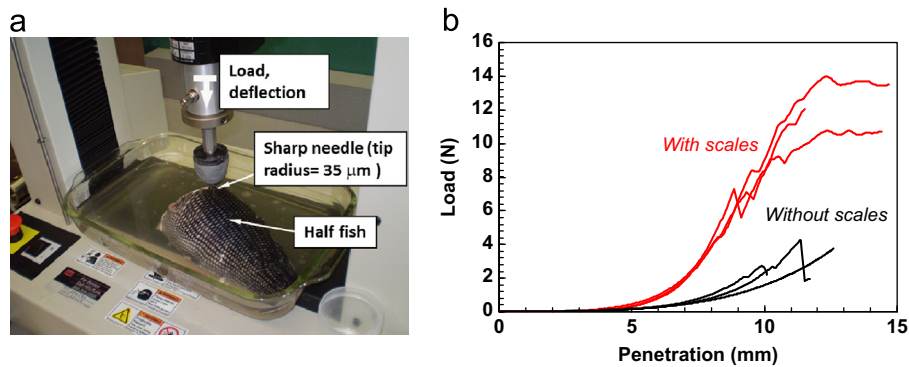


Fig. 3 – (a) Experimental setup for puncture tests on a half-striped bass; (b) force–displacement curves showing that the scales increase the puncture resistance of the skin by four to five times.

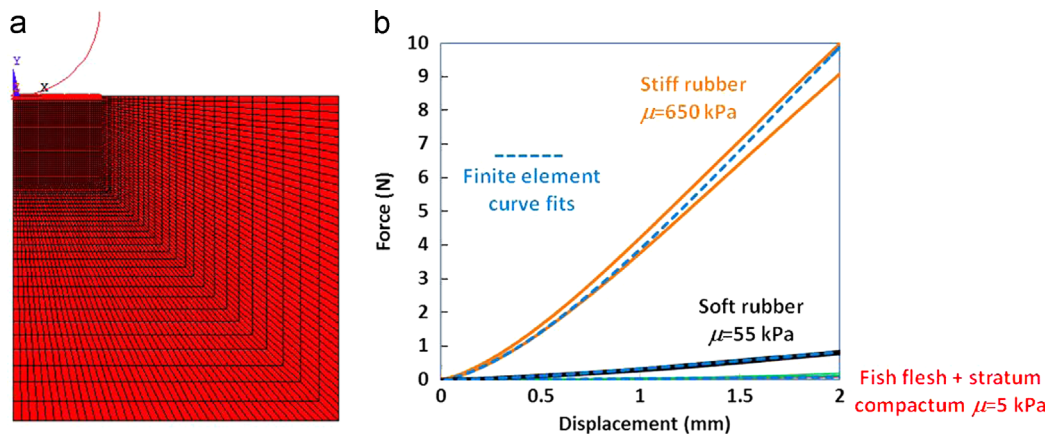
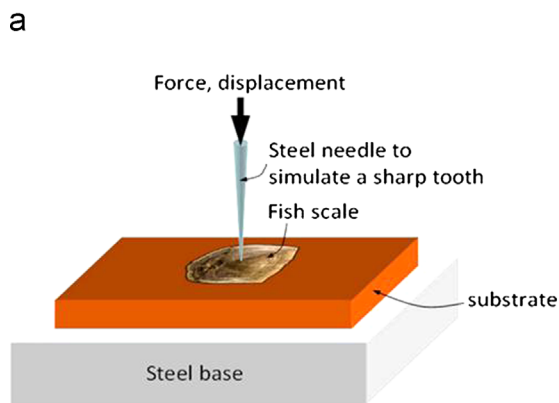


Fig. 4 – (a) Axisymmetric finite element model of the ball indentation test; (b) the model was used to fit the experimental curves, yielding the shear modulus of the Neo-Hookean substrates.

The experimental indentation curves were then fitted with the finite element model, with the shear modulus of the Neo-Hookean model μ as the fitting parameter. This model provided excellent fits to the experimental curves (Fig. 4b), and we found about an order of magnitude of difference between each of the three substrates in terms of stiffness. Individual fish scales ($E=0.5\text{--}1\text{ GPa}$, (Zhu et al., 2012)) are almost rigid in comparison: they are 10,000 times stiffer than the flesh and s. compactum. The three different substrates were then used for puncture tests on individual fish scales, following the setup and procedure described in Zhu et al. (Zhu et al., 2012). A sharp steel needle (tip radius = $25\ \mu\text{m}$) provided a good model for a tooth, with a simplified geometry and a stiffness about two orders of magnitude greater than the scales themselves (Zhu et al., 2012). The setup was installed in a miniature loading stage (Ernest F. Fullam Inc., Latham, NY, USA) in order to record force and displacement. These puncture tests were conducted in quasi-static conditions and at a relatively slow displacement rate of $0.005\ \text{mms}^{-1}$ (the effects of loading rate were not explored in this work). All of the tests were performed in hydrated conditions: the scales were stored in water and positioned on the substrate just before the test. The short duration of the test (several minutes) did not allow for significant loss of water content from evaporation, and specimens were kept hydrated throughout testing. Fig. 5 shows the results of this set of experiments. The stiffness of the substrate has, as expected, a strong effect on the stiffness and deflection during the puncture tests (Fig. 5a). However, we found that the substrate stiffness had no significant effect on the force required to puncture the scale, at least over the range of substrate stiffnesses explored here (which is consistent with the concept of a soft system protected by stiff scales). This finding therefore indicates that the puncture resistance (puncture force) of the fish skin remains unchanged whether the underlying substrate is contracted (stiff) or relaxed (soft). In terms of biomimetics, this result indicates that the stiffness of the backing material for artificial scales is of secondary importance. It is however important to limit the amount of deflection, at and around the puncture site, in order to minimize the risk of blunt injury to the underlying tissues. This aspect is discussed in further detail towards the end of this article.



5. Effect of puncture site

While previous puncture tests on individual fish scales were performed through the center of the scales (Meyers et al., 2012; Zhu et al., 2012), puncture performance probably depends, in fact, on the puncture location. To examine this effect, puncture tests were performed on a single fish scale at five different locations on the upper surface of the scale (Fig. 6a): midline distal (edge) locations in all four fields of the scale, i.e. anterior, posterior, dorso-lateral, and ventro-lateral edge locations, and a more central location within the anterior field near the elevated “focus”. The puncture force-displacement curves at each puncture site were highly repeatable, and showed a similar pattern with a slight force drop at $2.0\text{--}2.5\ \text{N}$ and a subsequent force increase until final failure (Fig. 6b). The puncture failure mode of a single scale follows the same mechanisms as discussed in (Zhu et al., 2012), regardless of puncture location. However, we observed differences in puncture stiffness and force across different puncture locations (Fig. 6b). The anterior center location had the highest puncture stiffness and force due to its increased thickness, and puncture force was lowest at the thin posterior edge location (Fig. 6c,d). The performance of the scale in resisting puncture was shown to be site dependent, which can be explained by variation in thickness across the scale (Fig. 2b) and possibly by other scale features, for example differences in HAp content and surface structures across the scale (Fig. 2a). As noted above, however, the “effective” thickness of protective material resulting from superposing three scales is uniform over the surface of the fish and as a result, puncture on whole fish was less dependent on location than for the individual scale.

6. Effect of number of overlapping scales

The scalation pattern generates overlap of scales which must all be defeated by a predator in order to injure the fish. In this section we explored potential synergies between scales when they overlap on the natural skin of fish. The same experimental setup as for the single scale test was used. As a first

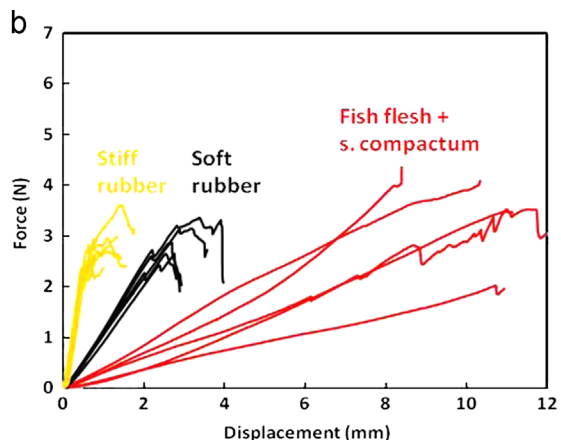


Fig. 5 – (a) Experimental setup for puncture tests on individual scales; (b) force–deflection curves for puncture tests using three different substrates.

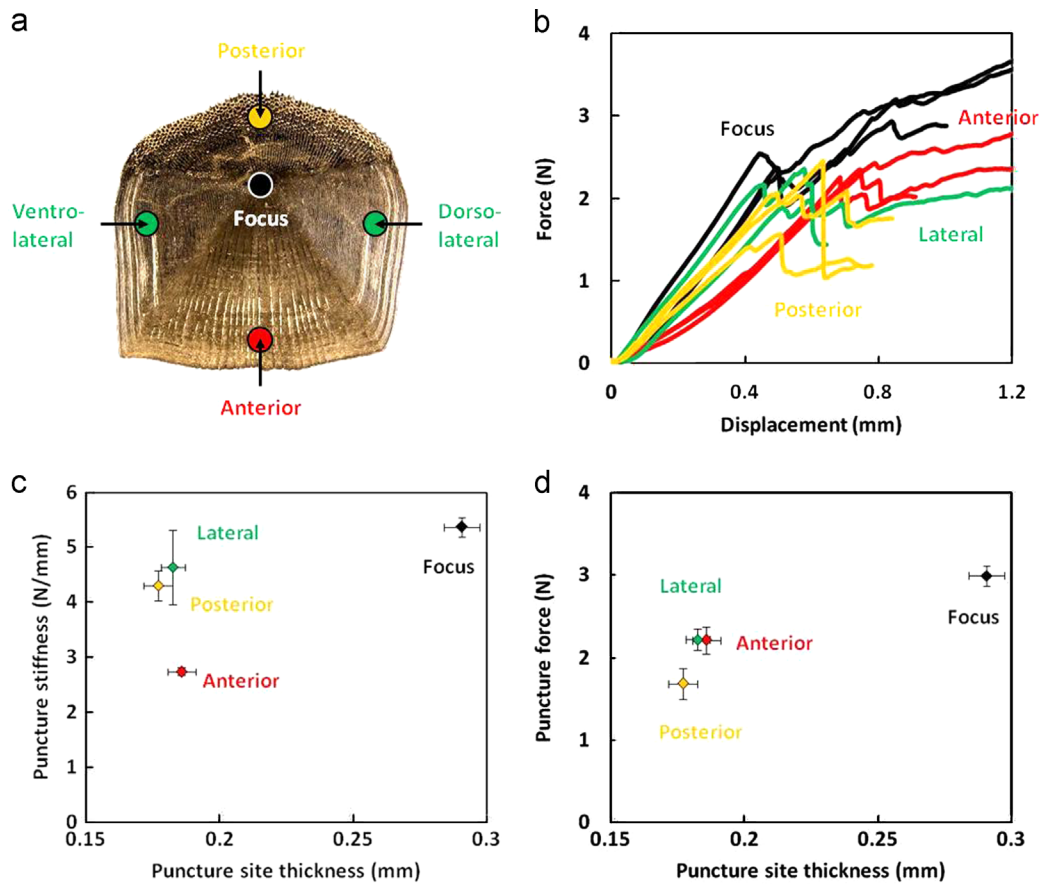


Fig. 6 – (a) Puncture sites on the scale including midline edge locations in the anterior, posterior and lateral fields, and a central location near the elevated “focus”; (b) force–displacement curves at each puncture site; (c) puncture stiffness as a function of puncture site thickness; (d) puncture force as a function of puncture site thickness.

set of experiments, we stacked several scales into piles up to ten scales thick on the hard rubber substrate (Fig. 7a). The scales were therefore completely overlapping one another and had the same orientation. A central location in the anterior area of the scale was targeted for puncture and the needle driven through the entire stack of scales. The force–displacement curves for stacks of 2, 3, 5 and 10 scales are shown in Fig. 7b, which also includes the force–displacement curve of individual scales. We found, as expected, that the force required to puncture the entire stack of scales increases with the number of scales. The failure mechanism was similar to what was observed for single scales (Zhu et al., 2012). The bony layers failed in sequence, softening the system while the underlying collagen layers delayed further penetration. Closer examination of the force–deflection curves revealed a sequence of softening/stiffening events corresponding to the needle defeating the bony layer (softening), and then deforming the collagen layer and meeting the upper surface of the next scale down (stiffening) until full penetration of each scale (“failure event”). These trends can be better seen by plotting the instantaneous stiffness (slope) of the force–deflection curve as a function of displacement (Fig. 7c).

Fig. 7d shows that the puncture force increases almost linearly with the number of scales, at least up to 3 scales, for example doubling the number of scales doubles the force at puncture. This result is relevant to striped bass since three

overlapping scales cover the body of the fish at any point. We found that for natural striped bass skin the mean puncture force value for the three scale overlap region was 6.90 ± 0.24 N ($n=5$), which is lower than the puncture force of three stacked scales (10.11 ± 0.25 N ($n=11$)) and can be explained by puncture site thickness. When the needle punctured 5 and 10 scales the results deviated from the linear trend, possibly due to the nonlinear profile of the needle. This result suggests that there are no significant synergistic mechanisms amongst scales in this configuration. Fig. 7b also shows that the puncture stiffness only slightly increased when the number of scales was increased: the scales are so much stiffer than the substrate that substrate deformation accounts almost entirely for the deflection measured here. In effect, the scale or stack of scales appeared to “sink” into the soft substrate over the course of the experiment. As a result, higher force to penetration resulted in more deflection at failure, as also shown in Fig. 7b. The effects of scale and substrate deflections are examined in more detail in Sections 8 and 9.

7. Effect of friction between scales

As discussed above, the upper surface of the scale is hard and shows intricate roughness patterns (circuli with denticles, Fig. 1d, and ctenii, Fig. 2a) which may generate friction or even possible mechanical locking between overlapping scales.

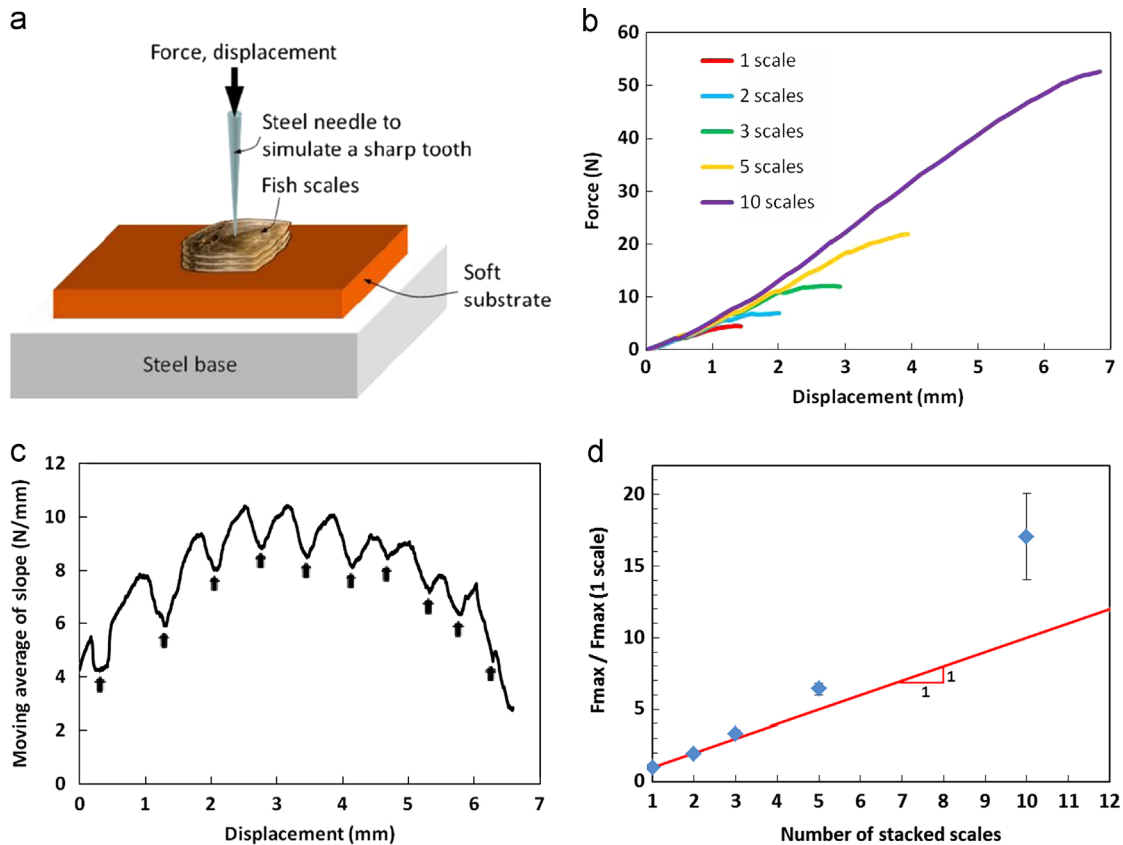


Fig. 7 – (a) Experimental setup for puncture tests on stacks of scales; (b) force–displacement curves; (c) instantaneous slope of the force–deflection curve as a function of displacement (arrows indicate scale “failure events”); (d) normalized puncture force as a function of number of stacked scales.

These interactions would increase puncture resistance and impact swimming performance. Friction coefficients can be challenging to measure experimentally for engineering materials, and even more so for a biological material like fish scales. In this work we therefore used an indirect approach which exploited the fact that the deformation of the scales during a puncture test is dominated by bending. In general, the bending stiffness of two or more stacked plates depends on how they are joined, and more specifically on what level of shear stresses can be transmitted at their interface. For example, a stack of perfectly bonded plates will have a significantly higher flexural stiffness compared to a stack of plates that are in simple, frictionless contact. We used this property to estimate the coefficient of friction between the scales. The initial stage of the puncture test was modeled with an axisymmetric finite element model (ANSYS Inc., Houston, Pennsylvania, USA). The model incorporated the salient features of the system: a Neo-Hookean substrate, scales including bony and collagen layers, and rigid indenter whose profile was built from optical images of the needle (Fig. 8a). The interface between the substrate and the scale was assumed to be frictionless, since both surfaces are smooth and hydrated. The experimental value for the stiffness of the hard rubber substrate was used in the model. Meanwhile, the properties of the bony and collagen layers within the scales were taken from previous experiments on striped bass scales (Zhu et al., 2012). Fig. 8b shows that the finite element model captures the initial slope of the

experimental puncture tests remarkably well (we limited the scope of this type of model to initial stiffness, because problems associated with element distortion and convergence appeared for large deflections).

In order to investigate the effect of friction between scales, additional finite element models were generated with stacks of 2, 3, 5, 8 and 10 scales (Fig. 8c). The friction parameter between the scales was the unknown in the models, and can be used as a parameter to fit the experiments. Two extreme cases were considered: perfectly bonded scales and frictionless scales. Fig. 8d shows the initial predicted slopes for these two types of interfaces and as function of number of scales. As expected, the initial stiffness increases with number of scales, and stacks of bonded scales are stiffer than frictionless scales. The initial stiffness from the experiments presented above is also plotted. The model does not exactly predict the experiments, possibly because the thickness of the scale in the model was assumed to be uniform without considering the actual conical shape of the scale (Fig. 2b). Nevertheless, the model suggests that the friction between the scales is negligible, since the frictionless models were the closest to the experiments. The circles therefore do not generate significant friction, probably because of the soft, gel-like, s. spongiosum between the scales, which may act as a solid lubricant, preventing direct contact between scales. Low friction between scales is highly beneficial in terms of swimming efficiency when the scales slide on one another, but may be less so in terms of puncture resistance.

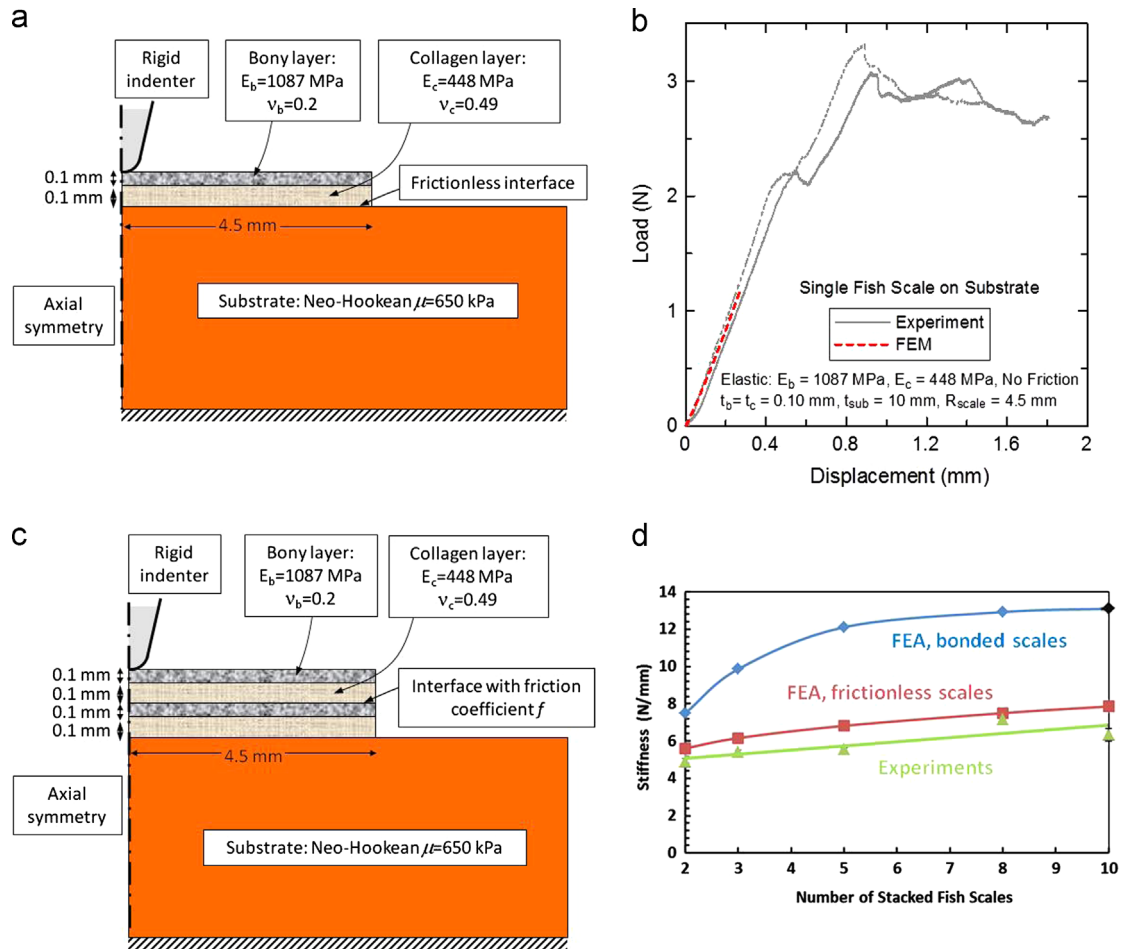


Fig. 8 – (a) Axisymmetric finite element model of a puncture test on a single scale; (b) comparison of the curves obtained by experiments and the FE model; (c) axisymmetric finite element model of a puncture test on a stack of 2 scales; (d) predicted (bonded and frictionless scales) and experimental initial slope of the force–deflection curve as a function of number of scales.

8. Effect of scale arrangement

The previous series of tests examined the puncture resistance of stacks of perfectly aligned scales. In reality, the scales overlap on the surface of the fish and the scalation pattern is more complex (Fig. 1b). To examine the effect of scale arrangement on overall puncture performance, three fish scales were plucked from the fish specimen and tested directly on the hard rubber substrate in three different arrangements (Fig. 9a): (i) stacked (which is the same arrangement as reported in the previous section), (ii) staggered overlap (which is the natural arrangement), and (iii) rotated (such that the “effective” protective thickness was the same as (ii)). The stacked scale arrangement was the same arrangement as reported in the previous section. It exhibited the thickest puncture site, the highest extent of scale overlap, and least of scale-substrate contact area. In the staggered overlap arrangement, three scales were arranged in the exact same pattern as the natural scalation pattern, and the puncture site was at the center of the overlapping region of the scales. The exposed areas of the scales were outlined with marker to facilitate replication of the natural overlap pattern directly on the rubber substrate. In the rotated arrangement, scale #2 was rotated 180° counter-clockwise and shifted down

or inserted entirely between scales #1 and 3 so that the dorso-ventral borders of all three scales were aligned and the three scales placed on the hard rubber substrate. The objective of the rotated configuration was to change the arrangement of the scales while maintaining the “effective” protective total thickness as the staggered overlap case.

Fig. 9b shows representative force–deflection curves for each of the three arrangements. We found that the stiffness was the same for all three arrangements, and that the staggered and rotated scales displayed the same penetration resistance, the final failure events corresponding to the slight force drops at the end of the force–displacement curves. The stacked scales, however, had the highest puncture resistance because the puncture site was in the anterior field of the stacked scales in a location that was notably thicker than the puncture sites for the staggered and rotated scale arrangements. Over the course of the tests on scales in different overlapping arrangements, we also made interesting observations: for all configurations, the stiff stacks of scales “sank” into the soft substrate (Fig. 9c). In the case of staggered overlap scales, the section of scales at the periphery of the system lost contact with the substrate. These two effects arose because of the large contrast of stiffness between the

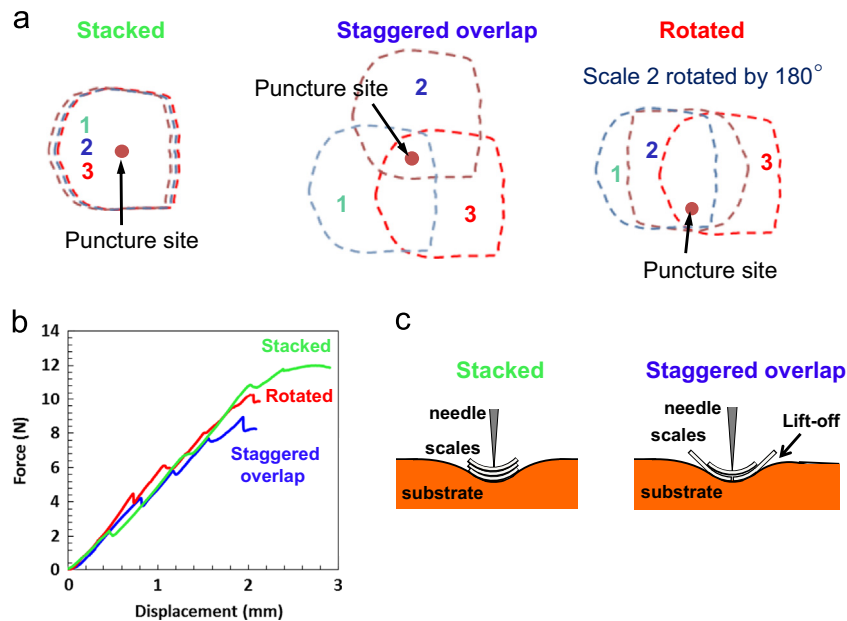


Fig. 9 – (a) The three scale arrangements used for puncture tests: stacked, staggered (natural) overlap, and rotated; (b) force–displacement curves for the three scale arrangements; (c) “sink-in” mechanism of scale and substrate deformation.

scales and the hard rubber substrate. The effective contact surface between scales and substrate remained essentially the same for all arrangements, and in all cases the scales appeared to “sink” within the soft substrate. This deformation mode resulted in high localized strains in the soft substrate, which would potentially lead to blunt injury on the actual fish. This observation motivated the final experiment in this study, where we investigated collective scale mechanisms around the puncture site.

9. Effect of scale interaction and force dispersal

The objective of this test was to assess the deflection of the skin during the puncture event on an actual fish, in order to unveil potential collective mechanisms of the scales preventing excessive deflection and localization. The overall experimental setup is shown in Fig. 10a. A whole fish was placed on a high capacity precision scale. A blunt probe (tip diameter=2.2 mm) attached to a micromanipulator, itself attached to a rigid column clamped on the table, was used to press onto the skin of the fish. The micromanipulator was used to impose deflections with accuracy, while the scale was used to measure the puncture force. For all tests, the loads were kept below the force required to penetrate the scales ($F=1$ N). Two cameras were mounted above the fish in order to image its surface from either side of the puncture site. These cameras produced stereo images of the fish skin (i.e. images of the same object viewed from two different points). The images were in turn used for three-dimensional image correlation (VIC-3D, Correlated Solutions, Inc.). This method can determine the three-dimensional shape of an object (in this case the surface of the fish). In addition, comparison of two pairs of images process the full three-dimensional displacement field (Fig. 10b). The correlation technique consists of tracking the location of dark and bright features on the

surface of the object, which we generated in this case by applying a finely crushed black graphite powder over the area surrounding the puncture site. The test consisted of acquiring a pair of initial images of the fish, and then acquiring another pair of images at a puncture force of 1 N. The test was first performed on an intact fish. The fish was then entirely descaled around the puncture site, except for the scale directly at the puncture site. The test was then repeated at the exact same location.

Fig. 11a shows the deflection of the fish skin around the puncture site for the scaled and descaled conditions. Profiles of these two surfaces were then taken along radial lines intersecting at the puncture site, in order to produce the plot shown on Fig. 11b. The results show that descaling the skin increases the deflection by about 25%, but only close to the puncture site. The region that showed additional deflection due to descaling corresponded to a circular area around the puncture site, whose size matched the dimensions of the scale. At larger distances of 10 mm and further away from the puncture site, the deflections of the scaled and descaled fish were similar. These observations confirmed the “sink-in” mechanism observed in the previous section (Fig. 9c). Individual scales subjected to localized puncture forces can deform the underlying soft tissues, possibly up to a point where the soft tissue is damaged. This type of “blunt trauma” is however averted by the surrounding scales, which support the scale being punctured and redistribute the puncture force over large surfaces and volumes in the soft tissue.

10. Conclusions

In this study, we showed that teleost fish scales, while being light and thin, provide a flexible layer with remarkable protection against sharp puncture. The resistance to puncture observed on the actual fish could be largely explained in light of the additional experiments and models we

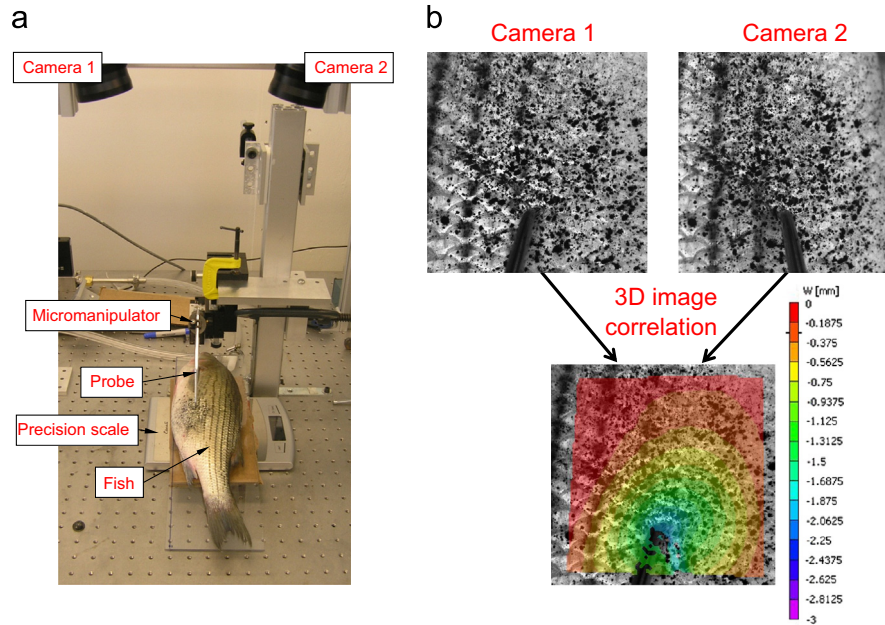


Fig. 10 – (a) Experimental setup for skin indentation tests on striped bass with stereo-imaging; (b) stereo images of the puncture site on the natural (scaled) fish at 1 N force, and 3D displacement field around the puncture site computed using 3D image correlation.

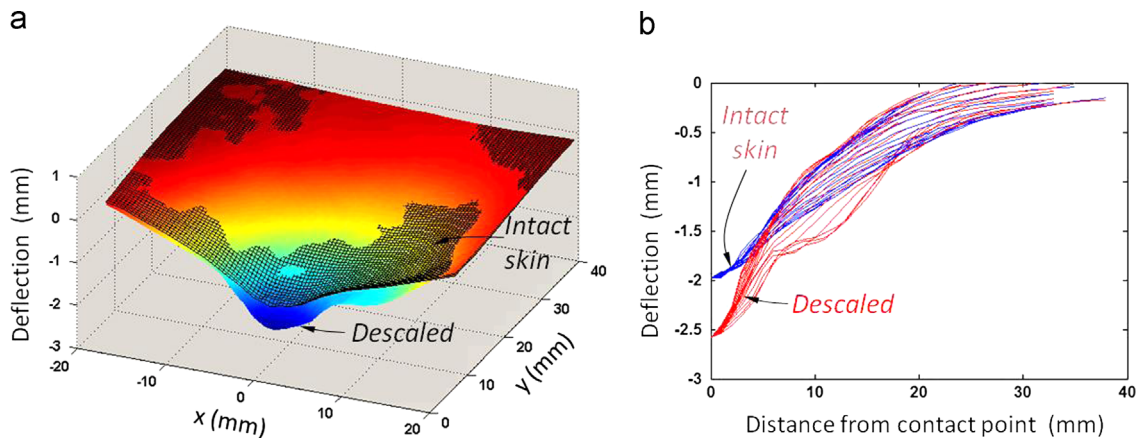


Fig. 11 – (a) Deflection of the skin around the puncture site for scaled and descaled conditions; (b) two-dimensional profiles around the puncture site for scaled and descaled conditions.

presented here. In summary, puncture resistance is generated by sophisticated mechanisms at the level of the individual scales, consisting of a two-step failure process involving both the bony layer and collagen layer. On the actual striped bass the scales form a well-defined scalation pattern, offering three layers of scales to resist puncture at any point on the fish. While there are significant variations in thickness within a given individual scale, the scalation pattern is such that the total “effective” protective thickness is uniform over the entire fish. The stiffness of the substrate was not found to affect the puncture force, at least in the range of substrate stiffnesses we explored (which are relevant to the actual fish and to actual biomimetic applications). We found that overlapping three scales essentially multiplies their puncture force by three. Friction between the scales is negligible, and therefore does not generate additional resistance to deformation and puncture, regardless of scale arrangement.

While our experiments and models demonstrate a rather simple scenario in terms of puncture force, they also revealed a new failure mode: even if the scales resist puncture, the large deflections and deformations of the softer underlying tissues around the puncture site may lead to blunt injury. Using stereo-imaging and image correlation, we demonstrated that the scales surrounding the puncture site redistribute the puncture force over large surfaces and volumes in the soft tissue, which verified a hypothesis we had proposed previously (Vernerey and Barthelat, 2010). This mechanism of scale interaction and force dispersal prevents unstable localized deformation of the skin and damage to underlying tissues. Fish scales therefore provide the fish with a flexible, light weight protective system against both laceration and blunt injuries. This study on natural fish skin teaches us useful lessons for future biomimetic “artificial fish scales”: the resistance to puncture of individual scales is

equally important as their overlap and their arrangement to provide efficient protection.

Acknowledgments

This project was supported by a grant from the National Science Foundation under award CMMI 0927585, and by a Discovery Grant from the Natural Sciences and Engineering Research Council of Canada. L.S. was partially supported by a McGill Engineering Doctoral Award from the Faculty of Engineering at McGill University. The authors would like to acknowledge the help and support of Mostafa Yourdkhani and Pascal Hubert for the initial puncture tests on whole fish. Histological processing was performed by Caroline Therien and Jo-Ann Bader (GCRC HC) at McGill University. Micro-CT scans were performed with the help of Trina Du, Redpath Museum and Dept. of Biology at McGill University. The three-dimensional image correlation imaging equipment and software was graciously provided by Luc Mongeau, and the authors would also like to acknowledge the help of his students Amir Miri, Hani Bakhshaei and Justin ChanWoo Yang.

REFERENCES

- Browning A., Ortiz C. and Boyce M.C. Mechanics of composite elasmoid fish scale assemblies and their bioinspired analogues. *Journal of the Mechanical Behavior of Biomedical Materials. Journal of the Mechanical Behavior of Biomedical Materials* 19, 2013, 75–86.
- Bruet, B.J.F., Song, J., Boyce, M.C., Ortiz, C., 2008. Materials design principles of ancient fish armour. *Nature Materials* 7, 748–756.
- Burdak V.D., 1979. Morphologie fonctionnelle du tegument ecailleux des poissons. Kiev: La Pensee Scientifique (in Russian). French Translation, *Cybium* 10, 1986, pp. 1–147.
- Elliott D.G., 2000. Chapter 5—Integumentary System (Gross Functional Anatomy), Chapter 17—Integumentary System (Microscopic Functional Anatomy). In: Ostrander, G.K., (Ed.), *The Laboratory Fish*, Academic Press, Oxford, England. pp. 95–108, 271–306.
- Marino Cugno Garrano, A., La Rosa, G., Zhang, D., Niu, L.-N., Tay, F.R., Majd, H., Arola, D., 2012. On the mechanical behavior of scales from *Cyprinus carpio*. *Journal of the Mechanical Behavior of Biomedical Materials* 7, 17–29.
- Hebrank, M.R., Hebrank, J.H., 1986. The mechanics of fish skin: lack of an "external tendon role in two teleosts". *Biological Bulletin* 171, 236–247.
- Ikoma, T., Kobayashi, H., Tanaka, J., Walsh, D., Mann, S., 2003. Microstructure, mechanical, and biomimetic properties of fish scales from *Pagrus major*. *Journal of Structural Biology* 142, 327–333.
- Lanzing, W.J.R., Higginbotham, D.R., 1974. Scanning microscopy of surface structures of *Tilapia mossambica* (Peters) scales. *Journal of Fish Biology* 6, 307–310.
- Meunier, F.J., Castanet, J., 1982. Organisation spatiale des fibres de collagene de la plaque basale des ecailles des Teleosteens. *Zoologica Scripta* 11, 141–153.
- Meyers, M.A., Lin, Y.S., Olevsky, E.A., Chen, P.-Y., 2012. Battle in the Amazon: *Arapaima* versus Piranha. *Advanced Engineering Materials* 14, B279–B288.
- Motta, P.J., 1977. Anatomy and functional morphology of dermal collagen fibers in sharks. *Copeia* 3, 454–464.
- Naresh, M.D., Arumugam, V., Sanjeevi, R., 1997. Mechanical behaviour of shark skin. *Journal of Biosciences* 22, 431–437.
- Schonborner, A.A., Boivin, G., Baud, C.A., 1979. The mineralization processes in teleost fish scales. *Cell and Tissue Research* 202, 203–212.
- Sire, J.Y., 1986. Ontogenic development of surface ornamentation in the scales of *Hemichromis bimaculatus* (Cichlidae). *Journal of Fish Biology* 28, 713–724.
- Torres, F.G., Troncoso, O.P., Nakamatsu, J., Grande, C.J., Gómez, C. M., 2008. Characterization of the nanocomposite laminate structure occurring in fish scales from *Arapaima gigas*. *Materials Science and Engineering C* 28, 1276–1283.
- Vernerey, F.J., Barthelat, F., 2010. On the mechanics of fishscale structures. *International Journal of Solids and Structures* 47, 2268–2275.
- Wainwright, S.A., Vosburgh, F., Hebrank, J.H., 1978. Shark skin: function in locomotion. *Science* 202, 747–749.
- Whitear, M., 1986. The skin of fishes including cyclostomes. In: Bereiter-Hahn, J., Matoltsy, A., Richards, K. (Eds.), *Biology of the Integument—2 Vertebrates*. Springer, Berlin, Germany, pp. 8–77.
- Yang, W., Chen, I.H., Gludovatz, B., Zimmermann, E.A., Ritchie, R. O., Meyers, M.A., 2013. Natural flexible dermal armor. *Advanced Materials* 25, 31–48.
- Zhu, D., Ortega, C.F., Motamedi, R., Szewciw, L., Vernerey, F., Barthelat, F., 2012. Structure and mechanical performance of a "modern" fish scale. *Advanced Engineering Materials* 14, B185–B194.